Title page

Title: High-altitude hypoxia exposure inhibits erythrophagocytosis by inducing macrophage ferroptosis in the spleen

Running title: Hypobaric hypoxia induces splenic ferroptosis

Type of article: Research article

Authors: *Wan-ping Yang[1△], Mei-qi Li[1△], Jie Ding[1], Jia-yan Li[1], Gang Wu[2,3], Bao Liu[2,3], Yu-qi Gao[2,3], Guo-hua Wang[1,4]*, Qian-qian Luo[1]**

[△]These authors contributed equally to this work.

Affiliations:

[1]Department of Physiology and Hypoxic Biomedicine, Institute of Special Environmental Medicine and Co-innovation Center of Neuroregeneration, Nantong University, 9 Seyuan Road, Chongchuan District, Nantong, Jiangsu 226019, China.

[2]College of High-Altitude Military Medicine, Institute of Medicine and Hygienic Equipment for High Altitude Region, Army Medical University, Chongqing 400038, China.

[3]Key Laboratory of Extreme Environmental Medicine and High-Altitude Medicine, Ministry of Education of China, Chongqing 400038, China.

[4]Department of Neurosurgery, Southwest Hospital, Army Medical University, Chongqing, Chongqing 400038, China

*Corresponding author: Guohua Wang, Email-address: wgh036@hotmail.com, ORCID: 0000-0002-4810-8534; or Qianqian Luo, Email-address: qianqianluo@ntu.edu.cn, ORCID: 0000-0001-8302-3117.

Abstract

High-altitude polycythemia (HAPC) occurs in high-altitude (HA) environments and involves an imbalance between erythropoiesis and eryptosis. Spleen/splenic macrophages are an important primary tissue/cell of eryptosis and iron recycling. However, the role of the spleen in the pathogenesis of HAPC and the effect of hypobaric hypoxia (HH) on the biology of the spleen and splenic macrophages are still unclear. We used a mouse hypobaric hypoxia (HH) exposure model to simulate an *in vivo* study of 6000 m HA exposure. For *in vitro* studies, we used a primary splenic macrophage model treated with 1% hypoxia. We found that the HH-treated mouse model promoted erythropoiesis and led to erythrocytosis. In addition, HH exposure resulted in marked splenic contraction followed by splenomegaly for up to 14 days. HH exposure impaired the red blood cell (RBC) handling capacity of the spleen, which was caused by a decrease in splenic macrophages in the red pulp. Moreover, HH treatment for 7 and 14 days promoted iron mobilization and ferroptosis in the spleen, as reflected by the expression of metabolism-related proteins and ferroptosis-related proteins. All of the protein expression levels were similar to the gene expression levels in human peripheral blood mononuclear cells. Single-cell sequencing of the spleen further demonstrated a significant decrease in macrophages in the spleen 7 days after HH exposure. In *in vitro* studies, we confirmed that primary splenic macrophages decreased and induced ferroptosis following hypoxic treatment, which was reversed by pre-treatment with the ferroptosis inhibitor ferrostatin-1. Taken together, HH exposure induces splenic ferroptosis, especially in red pulp macrophages, which further inhibits the clearance of

RBCs from the spleen. As such, it promotes the retention of RBCs in the spleen and causes splenomegaly, which may further lead to the persistent production of RBCs and ultimately to the development of HAPC.

Keywords: High altitude, Hypobaric hypoxia, High-altitude polycythemia, Spleen, Eryptosis, Ferroptosis

Background

A plateau is a special environment characterized by low atmospheric pressure and low partial oxygen pressure. Long-term exposure to plateau environments may lead to chronic mountain disease [1]. High-altitude polycythemia (HAPC) is a common and widespread chronic mountain sickness characterized by excessive erythrocytosis [2]. Hypobaric hypoxia (HH) is the main cause of erythrocytosis to alleviate hypoxic conditions in tissues under high-altitude (HA) exposure [3]. In a healthy organism, erythropoiesis in bone marrow is equivalent to eryptosis in the spleen [4]. Although HA/HH exposure can affect the balance between the formation and clearance of RBCs, a new physiological RBC steady state can be rapidly formed in normal individuals [5]. Nevertheless, RBC homeostasis is disturbed and never formed into a homeostasis status in HAPC patients, which finally results in a continuous increase in RBCs [4]. It is well known that HA/HH exposure may lead to erythropoiesis; however, the pathogenesis of eryptosis under HA/HH conditions remains unclear.

The spleen clears the altered RBCs in the circulation system, which helps to balance erythropoiesis and RBC clearance [6]. Moreover, red pulp macrophages (RPMs) of the

spleen are the major scavengers that remove unhealthy, old, and malformed RBCs from the circulation to recover iron [7]. In brief, RPMs recognize the RBCs to be removed through the signal on their cell surface and trigger RBC endocytosis and digestion into heme in lysosomes [8]. Subsequently, the heme is decomposed by heme oxygenase-1 (HO-1) into biliverdin, carbon monoxide and iron [9]. Most of the iron recycling from heme is transported out of the cell through ferroportin (Fpn) and then participates in the formation of RBCs through the combination of transferrin (Tf) and transferrin receptor (TfR) on the cell membrane [10]. A portion of the released iron is loaded into cellular ferritin (Ft; including Ft-H and Ft-L). Ft-H oxidizes Fe^{2+} (ferrous ion) to Fe^{3+} (ferric ion) in the presence of O_2, and then Fe^{3+} can be stored on Ft-L [11]. When the body's iron metabolism is vigorous, nuclear receptor coactivator 4 (NCOA4) can recognize Ft-H, bring Ft into the lysosomal pathway for degradation, and release iron in Ft for iron recycling in the body [12]. However, some iron is free in cells in the form of ferrous iron (Fe^{2+}), which is well known to be an important initiator of free radical oxidation. Moreover, the accumulation of large amounts of Fe^{2+} ions in cells may cause ferroptosis [13].

Although erythropoiesis under HA/HH is well studied thus far, the precise effects of HA/HH on erythrophagocytosis in the spleen remain largely unexplored. Based on the fact that the spleen is the major organ for RBC processing and that RPMs play an important role in recycling iron from RBC clearance, we investigated the effects of HA exposure on spleen/splenic macrophages in an HH-exposed mouse model (6000 m exposure conditions). In the current study, we further explored whether HA/HH could

regulate the erythrocyte disposal and iron recycling of macrophages, and specifically predict the damage of erythrophagocytosis after HA/HH exposure. We demonstrated that HH exposure induced ferroptosis in the spleen, especially in macrophages, which led to a decrease in the number of macrophages, followed by eryptosis and iron recycling in the spleen. These findings may be clinically relevant to continuous pathological erythrocytosis and HAPC progression under HA exposure.

Methods

HH mouse exposure model

Male C57BL/6 male mice (at 8 weeks of age) were obtained from the animal experimental centre of Nantong University. Mice were adapted to the facilities for 3 days before experiments. Mouse models of HH exposure were established by placing the mice in the decompression chamber (TOW-INT TECH, ProOx-810, China) for 1 d, 2 d, 3 d, 7 d, and 14 d. The parameters were set as follows: 6000 m above sea level, oxygen partial pressure of 11 kPa, lifting speed of 20 m/s, chamber pressure of 54 kPa, temperature of 25 °C, humidity of 40%, and 12-h light/dark cycles. Tuftsin (1.5 mg/kg, MCE, HY-P0240, USA) was used to stimulate the phagocytosis of macrophages and was injected at 7 d and 11 d during the 14-d period of mice exposed to HH.

Splenic macrophage culture and treatments

After isoflurane anaesthesia, mice were transcardially perfused with precooled PBS, and then splenic tissue (approximately 1mm^3 in volume) was collected and separated in cold, phenol red-free Hanks' balanced salt solution (HBSS; Gibco, Grand Island, NY, USA). The cell extracts were centrifuged at 500 rpm for 5 min at 4 °C. The pellets were

113 then resuspended and incubated with ammonium-chloride-potassium (ACK) lysing
114 buffer (Thermo Fisher Scientific, USA) for 3 min at room temperature. Next, cell
115 extracts were purified in a four-phase Percoll (Sigma–Aldrich, St. Louis, MO, USA)
116 gradient: 0, 30, 40, and 50% in HBSS. After centrifugation at 500 rpm for 20 min at
117 4°C, the macrophage-enriched fraction was collected at the interface between the 30%
118 and 40% phases. Cells were washed in two rounds with HBSS and then resuspended in
119 AIM V medium (Thermo Fisher Scientific). The cells in this medium were cultured at
120 37 °C and 5% CO_2 for 12 h. After the cells were treated with ferrostatin-1 (Fer-1, 2 μm;
121 Selleck Chemicals, S7243, USA) 1 h in advance, the cells were placed in a hypoxia
122 workstation (Invivo2, Ruskinn, UK) for 24 h.

123 **Blood smear and hematological indices**

124 The collected blood was gently mixed with EDTA (15 g/L) to obtain anticoagulant
125 blood, which was detected by a hematology analyser (XE-5000, Sysmex Corporation,
126 Japan). Blood smear preparation method: a blood sample is dropped onto a slide, and
127 another slide is used to push the blood sample into a uniform thin layer at a constant
128 speed. After the blood samples were dried, Wright's stain solution was added and
129 incubated for 1 min. Then, the slide was rinsed with water. Blood smears were
130 photographed with a DM4000B microscope (Leica, Germany).

131 **Western blot**

132 Tissue and cell samples were homogenized on ice after cell lysates and protease
133 inhibitors were added. Centrifugation was performed at 12,000 rpm for 15 min at 4°C
134 to collect the supernatant. Protein concentration was determined by the BCA detection

method. A sample containing 30 μg protein was loaded and run in each well of SDS–PAGE gels. The membranes were incubated with the following antibodies: HO-1 (1:2000, Abcam, ab13243, USA); Ft-L (1:1000, Abcam, ab69090, USA); Ft-H (1:1000, Novus, NBP1-31944, USA); NCOA4 (1:1000, Santa Cruz, sc-373739, USA); TfR (1:1000, Thermo Fisher, 13-6800, USA); Fpn (1:1000, Novus, NBP1-21502, USA); ACSL4 (1:1000, Santa Cruz, sc-271800, USA); xCT (1:1000, Proteintech, 26864-1-AP, USA); Gpx4 (1:1000, Abcam, ab125066, USA); CD206 (1:1000, RD, AF2535, USA); CD16 (1:2000, RD, AF1960, USA); and β-actin (1:1000, Sigma–Aldrich, A5316, USA). The secondary antibodies were as follows: goat anti-mouse (1:10000, Jackson, USA) and goat anti-rabbit (1:10000, Jackson, USA). The gray value of specific blots was scanned and analysed using ImageJ software (National Institute of Health, USA).

RT–PCR analysis

Total RNA extraction and RT–PCR analysis were performed essentially as described previously [14]. Primer sequences were as follows:

Gene	Primer sequence (5'-3')	Product length (bp)
Csf1	F: GGCTTGGCTTGGGATGATTCT R: GAGGGTCTGGCAGGTACTC	126
Csf2	F: GGCCTTGGAAGCATGTAGAGG R: GGAGAACTCGTTAGAGACGACTT	104
CCL2	F: TTAAAAACCTGGATCGGAACCAA R: GCATTAGCTTCAGATTTACGGGT	121
CCL7	F: GCTGCTTTCAGCATCCAAGTG R: CCAGGGACACCGACTACTG	135

152 **GEO analysis**

153 GSE46480 samples were found in the GEO database of NCBI with the keyword "High
154 Altitude" search. The data set was divided into two groups, one for the plain (Base
155 Camp) and the other for the plateau (Altitude), with a sample size of 98 for each group.
156 Blood samples were collected from the same person at McMurdo Station (48 m) and
157 immediately transferred to Amundsen-Scott South Pole Station (2835 m) on the third
158 day. R language was used for data analysis, and GraphPad Prism was used for statistics.

159 **Malondialdehyde (MDA), Cysteine (Cys) and Glutathione (GSH) content**
160 **detection**

161 MDA was detected by a Micro Malondialdehyde Assay Kit (Solarbio, BC0025, China).
162 Cys was detected by a Micro Cysteine Assay Kit (Solarbio, BC0185, China). GSH was
163 detected by a Micro Reduced Glutathione Assay Kit (Solarbio, BC1175, China).

164 **Immunofluorescence**

165 Frozen sections of the spleen (9 μm) were stored at -80°C. Sections were placed at room
166 temperature for 30 min before immunofluorescence staining, incubated in 10% BSA-
167 PBS for 10 min, incubated overnight with F4/80-PE (1:200, Biolegend, 123110, USA),
168 washed with 0.05% PBST three times, incubated with DAPI for 10 min, washed with
169 PBS three times, sealed with 50% glycerine-PBS, and photographed with a confocal
170 laser scanning microscope (SP8, Leica Microsystems, Wetzlar, Germany).

171 **Tissue iron staining (DAB-enhanced Perls' staining)**

172 DAB-enhanced Perls' staining for the spleen paraffin sections was performed as
173 described previously [15]. Briefly, the sections were washed with PBS and cultured in

174 freshly prepared Perls' solution (1% potassium ferricyanide in 0.1 M hydrochloric acid
175 buffer). The slides were then immersed and stained with DAB. All slides were
176 counterstained with hematoxylin and visualized under a DM4000B microscope (Leica,
177 Germany). Data were collected from three fields of view per mouse and
178 semiquantitatively analysed with ImageJ software. Quantitative results of iron staining
179 were finally normalized to the NN control group.

180 **Flow cytometry**

181 1) The steps of reticulocyte ratio detection were as follows: The experimental tube and
182 negative control tube were prepared, 125 μL normal saline, 4 μL anticoagulant and 125
183 μL TO working solution (1 μg/mL, Sigma, 390062, USA) were added to each tube, and
184 250 μL normal saline and 4 μL anticoagulant were added to each tube of the negative
185 control tube. After incubation at room temperature for 1 h, flow cytometry analysis was
186 carried out by using the FL1 (488 nm/525 nm) channel.

187 2) The steps for the determination of intracellular divalent iron content and lipid
188 peroxidation level were as follows: The spleen was made into a single cell suspension,
189 and then the RBCs were lysed. This step can be omitted from cell samples. A total of 1
190 $\times 10^6$ cells were incubated with 100 μL of BioTracker Far-red Labile Fe^{2+} Dye (1 mM,
191 Sigma, SCT037, USA) for 1 h or C11-Bodipy 581/591 (10 μM, Thermo Fisher, D3861,
192 USA) for 30 min. After the cells were washed with PBS twice, flow cytometry analysis
193 was carried out by using the FL6 (638 nm/660 nm) channel for determination of
194 intracellular divalent iron content or the FL1 (488 nm/525 nm) channel for
195 determination of lipid peroxidation level.

196 3) The steps for detecting the mortality of spleen cells and peritoneal macrophages
197 were as follows: 1×10^6 cells were incubated at room temperature for 40 min with 2
198 μM Calcein AM and 8 μM PI. Flow cytometry analysis was carried out by using FL1
199 (488 nm/525 nm, Calcein AM) and FL3 (488 nm/620 nm, PI) channels.
200 4) The steps for detecting the number of M1/M2 macrophages in the spleen were as
201 follows: 1×10^6 cells were incubated with 2% mouse serum-PBS for 10 min, incubated
202 with F4/80-PE (1:200), CD86-PE/Cyanine7 (1:20, Biolegend, 105014, USA), and
203 CD206-Alexa 647 (1:80, BD, 565250) for 30 min, and washed with 2% mouse serum-
204 PBS twice. Flow cytometry analysis was carried out by using FL2 (488 nm/575 nm,
205 F4/80- PE), FL5 (488 nm/755 nm, CD86- PE/Cyanine7) and FL6 (638 nm/660 nm,
206 CD206- Alexa 647) channels.
207 5) The steps for detecting the number of monocytes in blood, spleen and bone
208 marrow were as follows: 1×10^6 cells were incubated with 2% mouse serum-PBS for
209 10 min, incubated with F4/80-PE, CD11b-PE/CY7 (1:2000, BD, 552850, USA), and
210 Ly6C-APC (1:2000, Thermo Fisher, 17-5932-82) for 30 min, and washed with 2%
211 mouse serum-PBS twice. Flow cytometry analysis was carried out by using FL2 (488
212 nm/575 nm, F4/80- PE), FL5 (488 nm/755 nm, CD11b-PE/CY7) and FL6 (638 nm/660
213 nm, Ly6C-APC) channels.
214 **Phagocytosis of *E. coli* and RBCs**
215 *E. coli* was labelled with Cy5.5 (5 mg/mL), and RBCs were labelled with NHS-biotin
216 (20 mg/mL). Macrophages (1×10^6) were coincubated with *E. coli*-Cy5.5 or RBC-
217 Biotin for 30 min and washed with 2% mouse serum-PBS twice. Flow cytometry

218 analysis was carried out by using FL6 (638 nm/660 nm) to determine the phagocytosis
219 of spleen by *E. coli.* Macrophages (coincubated with Biotin-RBCs) were incubated with
220 streptavidin-FITC for 3 h and washed twice with 2% mouse serum PBS. FL1 (488
221 nm/525 nm) was used for flow cytometry analysis to determine the phagocytosis of
222 RBCs in the spleen.

223 **Single-cell RNA Sequencing**

224 The spleen tissues were surgically removed and stored in MACS Tissue Storage
225 Solution (Miltenyi Biotec, Bergisch Gladbach, Germany) until processing. Single-cell
226 dissociation was performed by the experimentalists at the GENECHEM laboratory
227 (Shanghai, China). Dissociated single cells were then stained for viability assessment
228 using Calcein-AM (BD Biosciences, USA) and Draq7 (BD Biosciences). The BD
229 Rhapsody system was used to capture transcriptomic information from single cells.
230 Single-cell capture was achieved by random distribution of a single-cell suspension
231 across >200,000 microwells through a limited dilution approach. Beads with
232 oligonucleotide barcodes were added to saturation so that a bead was paired with a cell
233 in a microwell. The cells were lysed in the microwell to hybridize mRNA molecules to
234 barcoded capture oligos on the beads. Beads were collected into a single tube for reverse
235 transcription and ExoI digestion. Upon cDNA synthesis, each cDNA molecule was
236 tagged on the 5′ end (that is, the 3′ end of an mRNA transcript) with a unique molecular
237 identifier (UMI) and cell barcode indicating its cell of origin. Whole transcriptome
238 libraries were prepared using the BD Rhapsody single-cell whole-transcriptome
239 amplification (WTA) workflow, including random priming and extension (RPE), RPE

240 amplification PCR and WTA index PCR. The libraries were quantified using a High
241 Sensitivity D1000 ScreenTape (Agilent) and High Sensitivity D1000 Reagents (Agilent)
242 on a 4150 TapeStation System (Agilent, Palo Alto, CA, USA) and the Qubit High
243 Sensitivity DNA assay (Thermo Fisher Scientific). Sequencing was performed on an
244 Illumina sequencer (Illumina Nova Seq 6000, San Diego, CA) in a 150 bp paired-end
245 run.

246 **Statistical analysis**

247 Statistical analysis was performed with GraphPad Prism 8.0 software. Two-tailed
248 Student's t test or one-way analysis of variance (ANOVA) with Tukey's post hoc test.
249 $P < 0.05$ was considered statistically significant.

250

251 ## Results

252 **HH exposure promotes erythrocytosis in mice**

253 To mimic 6000 m HA exposure, we placed C58BL/6 mice in an animal hypobaric
254 oxygen chamber and detected the blood indices in the blood of the mice after HH
255 exposure for different times. The blood smear showed that the number of RBCs was
256 increased from 3 to 14 days after HH exposure compared with the normobaric normoxia
257 (NN) group (Figure 1A). Routine blood tests further confirmed the results in blood
258 smears, which showed that the RBC number (Figure 1B), HGB content (Figure 1C) and
259 HCV value (Figure 1D) were all increased significantly to varying degrees, while MCH
260 was not changed after HH exposure (Figure 1E). We further performed flow cytometry
261 by TO staining to detect reticulocytes after 7 and 14 days of HH treatment. The results

262 showed that at both HH 7 and 14 d of exposure, the reticulocyte proportion was
263 increased (Figure 1F). In addition, the number of $CD47^+$ RBCs in the blood was also
264 significantly increased at both 7 (Figure 1G and H) and 14 days (Figure 1G and I) after
265 HH exposure. These results suggested that the HH-treated mouse model mimics HA
266 exposure well, which promotes erythropoiesis and results in erythrocytosis in mice
267 following HH exposure.
268
269 **Spleen inhibits the immoderate increase in RBCs under HH conditions**
270 To determine the roles of the spleen in RBC homeostasis under HA/HH, we
271 investigated the effects of HH on the morphology, volume and weight of the spleen as
272 well as erythrocyte indices. As shown in Figure 2, the spleen volume and weight were
273 decreased significantly after HH exposure for 1 day compared to NN treatment (Figure
274 2A-C). However, the spleen was obviously enlarged from 2 to 14 days after HH
275 exposure (Figure 2A-C). The results indicated that the spleen contracted, the stored
276 RBCs in the spleen were released into the blood at 1 day, and the RBCs were produced
277 and/or retained in the spleen from 2 to 14 days after HH exposure. In addition, we also
278 investigated the effect of the spleen on RBC homeostasis under HH conditions and
279 observed whether its clearance effect on RBCs in HH was compensated by the liver or
280 other mononuclear macrophage systems. We removed the spleen from mice using
281 splenectomies and then performed HH exposure for 14 days to detect the RBC counts
282 and blood deposition. The results showed that compared with the splenectomy group
283 mice under NN conditions or the sham group mice exposed to HH, erythrocyte

284 deposition (Figure 2D) and counts (Figure 2E), HGB (Figure 2F) and HCV (Figure 2G)
285 levels were all significantly increased 14 days after HH splenectomy, while MCH did
286 not change (Figure 2H). However, these indices were not changed in the mice with or
287 without splenectomies under NN conditions (Figure 2D and E). It is suggested that the
288 liver and other mononuclear macrophages did not play an effective compensatory role
289 under HH exposure conditions. In addition, the spleen is essential to maintain the
290 homeostasis of RBCs after HH exposure, which can inhibit the excessive proliferation
291 of RBCs after HH exposure.
292
293 **HH exposure causes a decrease in the number of macrophages in spleen**
294 Since macrophages are the main cell population for processing RBCs in the spleen
295 under physiological conditions, we next investigated the counts and activity of
296 macrophages after 7 or 14 days of HH exposure via single-cell sequencing and flow
297 cytometry. Single-cell sequencing of the spleen showed that splenic macrophages were
298 significantly decreased after 7 days of HH exposure (Figure 3A-C). Moreover, the flow
299 cytometry of Calcein/PI double staining showed that the living cells of spleen were
300 significantly decreased while the dead cells were significantly increased after HH
301 exposure for 7 and 14 days (Figure 3D-F). We further found that both CD16 (M1
302 macrophage marker) and CD206 (M2 macrophage marker) expression were decreased
303 at both 7 and 14 days of HH exposure (Figure 3G-L). The flow cytometry results were
304 also consistent with the Western blot results, which showed that mature macrophages
305 ($F4/80^+/CD11b^+$), including M1-type ($F4/80^+/CD86^+$) and M2-type ($F4/80^+/CD206^+$)

306 macrophages, in the spleens of mice decreased after HH exposure for 14 days (Figure
307 3M). Next, to identify the migration and differentiation of monocytes from bone
308 marrow to spleen, we further analysed the expression of chemokines CCL2, CCL7,
309 Csf1 and Csf2 in spleen by qPCR and detected the number of monocytes in bone
310 marrow and spleen by flow cytometry. The results showed that CCL2 and CCL7 (Figure
311 3N) and Csf1 and Csf2 (Figure 3O) expression were significantly decreased in the
312 spleen after HH exposure at 7 and 14 days. Moreover, monocytes ($Ly6C^{+}/CD11b^{+}$) in
313 the bone marrow (Figure 3P-R) and spleen (Figure 3P and S-T) also declined after HH
314 for 7 and 14 days. Then, we assessed macrophage depletion in the spleen under HH via
315 detection of the expression and distribution of HO-1 and F4/80. Figure 3U shows that
316 both HO-1 and F4/80 were distributed in the red pulp of the spleen, and their expression
317 was also decreased after HH exposure. These results suggested that the number of
318 splenic macrophages decreased after HH exposure, resulting in the impairment of the
319 processing ability of splenic erythrocytes.
320
321 **HH exposure decreases erythrophagocytosis and the iron processing capacity of**
322 **the spleen**
323 We further investigated the effects of HH exposure on erythrocyte phagocytosis and
324 heme iron recycling in splenic macrophages. We used Cy5.5 dye to label *E. coli* (Figure
325 4A) and incubated them with splenic cells from HH-exposed mice *in vitro*, and the
326 phagocytosis of splenic cells was detected using flow cytometry (Figure 4B). Figure
327 4B shows that the phagocytic ability of splenic cells *in vitro* was significantly decreased

328 after 7 days of HH exposure. In addition, we used biotin to label autologous RBCs and
329 injected them into mice followed by HH treatment *in vivo* (Figure 4C and D), and the
330 phagocytosis of splenic cells was detected using flow cytometry. At 7 and 14 days after
331 HH, the number of biotin-labelled RBCs in blood and spleen cells decreased
332 significantly (Figure 4E-H). Although the labelled RBC decay declined automatically
333 with time, the degree of RBC decay in the HH exposure group was weaker than that in
334 the NN group in both the blood (Figure 4E and G) and spleen (Figure 4F and H).
335 Compared with blood, the phagocytic ability of mouse spleen macrophages to RBCs
336 decreased more significantly after HH exposure, especially on the 14th day (Figure 4G
337 and H). Furthermore, we injected Tuftsin, which can stimulate phagocytosis of
338 macrophages, and performed immunofluorescence and iron staining to study the heme
339 iron recycling ability of the spleen under HH conditions (Figure 4I). As shown in Figure
340 4J, compared with the NN group, F4/80 expression was decreased significantly as well
341 as Fe^{3+} deposition in the red pulp after HH exposure. However, Tuftsin induced F4/80
342 expression and Fe^{3+} deposition in the red pulp of the spleen under HH (Figure 4K and
343 L). These results suggested that the erythrocyte phagocytosis and heme iron recycling
344 ability of the spleen were suppressed, which was mainly due to the decrease in
345 macrophages in red pulp under HH conditions.
346
347 **HH exposure promotes iron mobilization and induces ferroptosis in the spleen**
348 To clarify the precise mechanisms of macrophage reduction caused by HH, we
349 examined the expression of iron metabolism- and ferroptosis-related proteins in mice

350 treated with HH and analysed the expression of the corresponding genes in peripheral
351 blood mononuclear cells (PBMCs) of healthy people acutely exposed to an HA
352 environment from GEO data (No. GSE46480). The results showed that compared to
353 the NN group, the expression levels of HO-1, Ft-L, Ft-H, NCOA4, and xCT were
354 decreased, while the expression levels of Fpn, TfR and ACSL4 were significantly
355 increased both at 7 and 14 days following HH exposure (Figure 5A-B, D-E; Figure S1,
356 A-D). Except for NCOA4, the expression changes in iron metabolism and ferroptosis
357 genes in PBMCs were consistent with our WB results (Figure 5C and F). There were
358 no significant changes in the expression of the GPX4 gene and protein in human
359 PBMCs and mouse spleens. The changes in iron metabolism- and ferroptosis-related
360 genes in PBMCs can fully reflect the protein changes in the spleen under HH exposure.
361 The levels of Fe^{2+} and lipid ROS in the spleen were detected by flow cytometry, and
362 the contents of MDA, GSH and Cys were detected by biochemical detection kits. As
363 shown in Figure 5G and H; Figure S1I-K, the levels of Fe^{2+} (Figure 5G; Figure S1E
364 and F) and lipid ROS (Figure 5H; Figure S1G and H) in the spleen were significantly
365 increased after HH exposure. In addition, the content of MDA (Figure 5I; Figure S1I)
366 in the spleen was increased, while Cys (Figure 5J; Figure S1J) and GSH (Figure 5K;
367 Figure S1K) were decreased significantly after HH exposure. All these results
368 suggested that iron mobilization in the spleen was enhanced and ferroptosis was then
369 induced after 7 days of HH exposure.
370
371 **Hypoxia promotes ferroptosis of primary splenic macrophages**

372 To study whether hypoxia exposure can induce ferroptosis in macrophages, changes in
373 Fe^{2+} and lipid ROS levels, cell viability, phagocytosis and ferroptosis-related protein
374 expression in primary splenic macrophages were detected under hypoxia in the
375 presence of a ferroptosis inhibitor (Fer-1). As shown in Figure 6, compared with the
376 normoxia control group (Nor), the levels of Fe^{2+} (Figure 6A-C) and lipid ROS (Figure
377 6D-E) were significantly increased, and the number of viable cells (Figure 6G-H) and
378 phagocytosis ability (Figure 6I) were also significantly increased after 24 h of hypoxia
379 (Hyp) treatment. In addition, with prolonged hypoxia time, the expression of ACSL4
380 gradually increased, while the expression of xCT and GPX4 decreased (Figure 6F). Fer-
381 1 inhibited the increase in Fe^{2+} content (Figure 6J-K) and reversed the expression
382 changes in ACSL4, xCT and GPX4 caused by hypoxia exposure (Figure 6L-O). At the
383 same time, Fer-1 reversed the levels of MDA, Cys and GSH induced by hypoxia (Figure
384 6P-R). These results confirmed that hypoxia induced ferroptosis in primary splenic
385 macrophages.
386

387 **Discussion**

388 The purpose of this study was to explore the effects and mechanisms of HA/HH
389 exposure on erythrophagocytosis and iron circulation in mouse spleens. Here, we used
390 an HH chamber to simulate 6000 m HA exposure and found that HH exposure induced
391 iron mobilization and activated ferroptosis in the spleen, especially in red pulp
392 macrophages (RPMs), which subsequently inhibited the phagocytosis and clearance of
393 RBCs. Finally, chronic exposure to HA/HH may promote the retention of RBCs in the

394 spleen, cause splenomegaly, advance RBC production, and promote the occurrence and
395 development of HAPC (Figure 7).
396 RBCs/erythrocytes are the carriers of oxygen and the most abundant cell type in the
397 body. Erythrocytes are rapidly increased by triggering splenic contraction in acute
398 HA/HH exposure [16] and stimulating erythropoiesis in subsequent continuous or
399 chronic HA/HH exposure. Changes in spleen morphology and size are closely related
400 to the spleen's ability to recover RBCs [17], and studies have shown that the spleen is
401 in a contraction state after short-term exposure to HA/HH, and approximately 40% of
402 the increase in RBCs is due to the contraction of the spleen [16, 18, 19]. In the present
403 study, mice were treated under HH to mimic HA exposure (mainly mimicking the low
404 oxygen partial pressure environment of 6000 m HA) for different times according to
405 other studies [20, 21]. Our results showed that HH exposure not only significantly
406 increased the RBC and HGB contents but also significantly increased $CD47^{+}$ cells in
407 blood. However, short-term (1 d) HH exposure caused spleen contraction and induced
408 splenomegaly after 3 d of HH treatment. These results are consistent with other research
409 results; that is, HH or HA exposure affects spleen morphology and further affects RBC
410 counts and HGB levels [22-24].
411 HAPC is a common chronic HA disease characterized by excessive proliferation of
412 RBCs caused by HH conditions [25]. Under physiological conditions, RBC
413 homeostasis is maintained by balancing erythropoiesis and erythrocyte clearance [4].
414 The ability of RBC disposal in the spleen for iron recycling under HA/HH exposure
415 was important to RBC regeneration in bone marrow (BM) [26]. Thus, we hypothesized

416 that erythrophagocytosis and iron recycling in the spleen were altered by HA/HH
417 exposure and further disturbed RBC homeostasis and affected the progression of HAPC.
418 We found that compared with sham group mice, HH significantly increased the contents
419 of RBCs and HGB in the blood of splenectomy mice. This strongly verified that the
420 spleen is a key organism that maintains RBC magnitude within a certain range of
421 physiological statuses under HA/HH conditions.

422 As originally proposed by Metchnikoff in the 19th century, macrophages, especially
423 RPMs, play a pivotal role in the regulation of RBCs and iron homeostasis [27, 28]. We
424 detected the macrophage population in the spleen and found that HH exposure for 7
425 and 14 days reduced the total macrophage and M1- and M2-type macrophage
426 proportions in the spleen. This result is supported by another study, that is, hypoxia
427 reduces M1-type macrophages in human gastric cancer [29]. We next observed whether
428 monocyte migration and differentiation from the BM to the spleen replenish reduced
429 macrophages and sustain macrophage homeostasis after HH treatment. It is well known
430 that splenic erythropoiesis is a dynamic process [4]. Upon phagocytosing erythrocytes
431 in macrophages, spleen tissue (including macrophages and fibroblasts) produces the
432 chemokine C–C motif chemokine ligand 2 and 7 (CCL2 and CCL7) to recruit blood
433 monocytes to the spleen [30, 31]. Unlike most studies in tumours, which mainly
434 suggested that macrophage accumulation in hypoxic areas was derived by enhanced
435 chemokine expression in tumours [32, 33], CCL2, CCL7 and Csf1 expression was
436 decreased in the spleen after HH exposure for 7 and 14 days in our study. Furthermore,
437 we found that HH exposure inhibited Ly6C^{hi} monocyte migration from the BM to

438 spleen, where these cells subsequently differentiated into RPMs. The combination of
439 decreased splenic RPMs, along with the reduced BM-derived Ly6C^{hi} monocytes,
440 suggests that the homeostasis of the RPM population of circulating monocytes was also
441 inhibited after the RPM depletion induced by HH exposure.

442 HO-1 is a major antioxidant and cytoprotective enzyme that catalyzes the
443 degradation of heme to provide heme homeostasis and protect against free heme-
444 induced toxicity [34]. In addition, it was supposed that mice deficient in HO-1 are
445 largely devoid of RPMs and suggested that HO-1 is critical for RPM development and
446 survival after erythrocyte clearance [35]. The reduced HO-1 protein of red pulp in our
447 study also implied decreased macrophage accounts induced by HH exposure, although
448 HO-1 was considered to be upregulated by hypoxia-inducible factor 1 (HIF-1) under
449 hypoxia [36, 37]. Along with the decreased macrophage amount induced by HH, the
450 phagocytic ability of macrophages in the spleen was also inhibited both *in vitro* and *in*
451 *vivo*. Meanwhile, the injection of tufftsin strongly confirmed the enhancement of heme
452 iron processing in the spleen under HH exposure. Nevertheless, our data conflict with
453 the study of Anand *et al*, which reported that hypoxia causes an increase in phagocytosis
454 by macrophages in a HIF-1α-dependent manner [38]. This may be because they
455 performed intermittent hypoxia, while we used consistent hypoxia in the present study.

456 The central role played by macrophages in supporting erythrocyte homeostasis stems,
457 in part, from digesting the HGB content of clearance RBCs and recycling the iron back
458 to erythroid progenitors for heme synthesis and HGB production [39]. In mammals, the
459 majority of the body iron is in the form of heme, and the largest pool of heme consists

460 of HGB [40]. HGB contains four prosthetic hemoglobins, and each mature RBC is
461 thought to contain approximately 1.2×10^9 heme moieties [39]. As previously
462 mentioned, the majority of iron required to sustain erythropoiesis is derived from
463 recycled RBCs. In general, RPMs are equipped with molecular machinery capable of
464 neutralizing the toxic effects of heme and metabolizing iron [41, 42]. Nevertheless,
465 defects in erythrocytophagy in macrophages probably lead to aberrant iron metabolism,
466 including anemia and iron overload [41]. The release of heme upon processed RBCs
467 constitutes a permanent and considerable threat for iron cytotoxicity in macrophages
468 and may eventually result in a specific form of programmed cell death termed
469 ferroptosis [43], which may cause decreased cell counts [44, 45].

470 Accordingly, we investigated the iron metabolism status and explored ferroptosis in
471 spleen/macrophages after HH/hypoxia treatment and found that HH exposure prompted
472 iron mobilization, especially in ferritinophagy and lipid peroxidation in the spleen.
473 Interestingly, we found that except for NCOA4, all the gene expression changes in the
474 PBMCs of humans after acute HA exposure were similar to the changes in the spleens
475 of mice after HH exposure for 7 and 14 days. This is probably because NCOA4 in the
476 spleen mediates iron release from Ft-L and facilitates iron reuse, while PBMCs do not
477 possess this function *in vivo*. These results not only indicated that HH exposure induces
478 spleen ferroptosis but also implied that the gene expression changes in PBMCs under
479 HA/HH may reflect RBC processing functions in the spleen and further indicate the
480 iron metabolism status in the clinic. We further found that the exact mechanism of
481 macrophage ferroptosis induced by HH exposure was caused by increased Fe^{2+} and

482 decreased antioxidative system expression, which finally resulted in lipid peroxidation
483 of macrophages. It has been proposed that heme catabolism by HO-1 protects
484 macrophages from oxidative stress [41]. The enhanced ROS and lipid peroxidation *in*
485 *vivo* were also consistent with the decreased HO-1 expression in the spleen. In addition,
486 1% hypoxia treatment induced ferroptosis *in vitro*, which was reduced by treatment
487 with ferrostatin-1, a ferroptosis inhibitor. However, our data were inconsistent with the
488 study of Fuhrmann *et al*., which reported that hypoxia inhibits ferritinophagy and
489 protects against ferroptosis [46]. We hypothesized that the enhanced iron demand for
490 new RBC regeneration in BM caused by HH leads to an increase in NCOA4 and Ft-L
491 protein expression in the spleen. On the other hand, hypoxia inhibited anti-ferroptosis
492 system expression, including reduced Gpx4 expression and increased lipid ROS
493 production. The results were supported by the group of Youssef LA *et al*, who reported
494 that increased erythrophagocytosis induces ferroptosis in RPMs in a mouse model of
495 transfusion [47]. However, as most studies have reported, ferroptosis is not only
496 characterized by increased lipid ROS but also significantly shrinking mitochondria [48].
497 We never found shrinking mitochondria in RPMs after HH exposure (data not shown).
498 Gao *et al*. proposed that mitochondria played a crucial role in cysteine deprivation-
499 induced ferroptosis but not in that induced by inhibiting glutathione peroxidase-4
500 (GPX4), the most downstream component of the ferroptosis pathway [49]. Interestingly,
501 in our *in vivo* study, Gpx4 expression was also not changed after HH exposure. It is still
502 not clear whether mitochondria are involved in ferroptosis. Whether HH treatment
503 caused mitochondrial swelling directly and the exact mechanism involved in this

process still need to be further investigated.

Based on the above experiments, we first put forward the "spleen theory" of HAPC (Figure 7). It hypothesizes that HH exposure induced spleen ferroptosis, especially RPMs, which further inhibited erythrophagocytosis, RBC clearance, HGB processing and iron recycling. Therefore, chronic exposure to HA/HH promotes the retention of RBCs in the spleen, leading to splenomegaly and the continuous production of RBCs. These findings may be clinically relevant to the pathological conditions of HAPC progression.

Abbreviations

BM: bone marrow; Cys: Cysteine; GSH: Glutathione; Ft-L: Ferritin light chains; Fpn: Ferroportin; Ft: Ferritin; HH: Hypobaric hypoxia; HA: High-altitude; HAPC: High-altitude polycythemia; HO-1: Heme oxygenase-1; HCT: Haematocrit; HGB: Haemoglobin; HIF-1a: Hypoxia inducible factor 1 a; MCH: Mean corpuscular haemoglobin; MDA: Malondialdehyde; NN: Normobaric normoxia; NCOA4: nuclear receptor coactivator 4; PBMCs: peripheral blood mononuclear cells; RBC: Red blood cell; RPM: Red pulp macrophage; TfR1: Transferrin receptor 1; Tf: Transferrin; TfR: Transferrin receptor.

Author contributions

QQL and GHW conceived, organized, and designed the study. YQG supervised the

work. WPY, MQL, JD and JL performed the experiments. WPY, GW and BL contributed to the analysis of data. QQL and GHW prepared, wrote and revised the manuscript. All authors contributed to read, and approved the submitted version.

Funding

This work was supported by Natural Science Foundation of China (Grants 32271228, 82171190, and 81873924), Open Cooperation Program from Key Laboratory of Extreme Environmental Medicine, Ministry of Education (KL2019GY011), China Postdoctoral Science Foundation (2020M673649), High-level Innovation and Entrepreneurship Talents Introduction Program of Jiangsu Province of China, and Nantong Municipal Science and Technology Project (MS12021020 and MS22021010).

Availability of data and materials

The datasets used and/or analyzed during the current study are available from the corresponding author on reasonable request.

Declarations

Ethics approval and consent to participate

All animal care and experimental protocols were carried out according to the Chinese Animal Management Rules of the Ministry of Health and were authorized by the Animal Ethics Committees of Nantong University research program protocol #S20190219-011. The results of the study are presented clearly, honestly, and without

fabrication, falsification, or inappropriate data manipulation.

Consent for publication

Not applicable.

Competing interests

The authors have no relevant financial or non-financial interests to disclose.

Author details

[1]Department of Physiology and Hypoxic Biomedicine, Institute of Special Environmental Medicine and Co-innovation Center of Neuroregeneration, Nantong University, 9 Seyuan Road, Chongchuan District, Nantong, Jiangsu 226019, China. [2]College of High-Altitude Military Medicine, Institute of Medicine and Hygienic Equipment for High Altitude Region, Army Medical University, Chongqing 400038, China. [3]Key Laboratory of Extreme Environmental Medicine and High-Altitude Medicine, Ministry of Education of China, Chongqing 400038, China. [4]Department of Neurosurgery, Southwest Hospital, Army Medical University, Chongqing, Chongqing 400038, China.

References

1. Pérez-Padilla R. Impact of moderate altitude on lung diseases and risk of high altitude illnesses. Revista de investigacion clinica; organo del Hospital de Enfermedades de la Nutricion. 2022;74(5):232-43.
2. Liu X, Zhang H, Yan J, Li X, Li J, Hu J, et al. Deciphering the Efficacy and Mechanism of Astragalus membranaceus on High Altitude Polycythemia by Integrating Network Pharmacology and In Vivo Experiments. Nutrients. 2022;14(23).
3. Tymko MM, Lawley JS, Ainslie PN, Hansen AB, Hofstaetter F, Rainer S, et al. Global Reach 2018 Heightened α-Adrenergic Signaling Impairs Endothelial

Function During Chronic Exposure to Hypobaric Hypoxia. Circulation research. 2020;127(2):e1-e13.
4. Dzierzak E, Philipsen S. Erythropoiesis: development and differentiation. Cold Spring Harb Perspect Med. 2013;3(4):a011601.
5. Robach P, Hansen J, Pichon A, Meinild Lundby AK, Dandanell S, Slettaløkken Falch G, et al. Hypobaric live high-train low does not improve aerobic performance more than live low-train low in cross-country skiers. Scandinavian journal of medicine & science in sports. 2018;28(6):1636-52.
6. Qiang Y, Sissoko A, Liu ZL, Dong T, Zheng F, Kong F, et al. Microfluidic study of retention and elimination of abnormal red blood cells by human spleen with implications for sickle cell disease. Proc Natl Acad Sci U S A. 2023;120(6):e2217607120.
7. Wirth F, Lubosch A, Hamelmann S, Nakchbandi IA. Fibronectin and Its Receptors in Hematopoiesis. Cells. 2020;9(12).
8. Slusarczyk P, Mandal PK, Zurawska G, Niklewicz M, Chouhan K, Mahadeva R, et al. Impaired iron recycling from erythrocytes is an early hallmark of aging. eLife. 2023;12.
9. Nemeth E, Ganz T. Hepcidin-Ferroportin Interaction Controls Systemic Iron Homeostasis. Int J Mol Sci. 2021;22(12).
10. Hidalgo D, Bejder J, Pop R, Gellatly K, Hwang Y, Maxwell Scalf S, et al. EpoR stimulates rapid cycling and larger red cells during mouse and human erythropoiesis. Nat Commun. 2021;12(1):7334.
11. Wang W, Grier DD, Woo J, Ward M, Sui G, Torti SV, et al. Ferritin H is a novel marker of early erythroid precursors and macrophages. Histopathology. 2013;62(6):931-40.
12. Bellelli R, Federico G, Matte' A, Colecchia D, Iolascon A, Chiariello M, et al. NCOA4 Deficiency Impairs Systemic Iron Homeostasis. Cell Reports. 2016;14(3):411-21.
13. von Krusenstiern AN, Robson RN, Qian N, Qiu B, Hu F, Reznik E, et al. Identification of essential sites of lipid peroxidation in ferroptosis. Nature chemical biology. 2023.
14. Luo Q, Hu J, Yang G, Yuan X, Chen Z, Wang D, et al. Fasting Increases Iron Export by Modulating Ferroportin 1 Expression Through the Ghrelin/GHSR1alpha/MAPK Pathway in the Liver. Biol Trace Elem Res. 2021;199(1):267-77.
15. Jiang H, Zhang X, Yang W, Li M, Wang G, Luo Q. Ferrostatin-1 Ameliorates Liver Dysfunction via Reducing Iron in Thioacetamide-induced Acute Liver Injury in Mice. Frontiers in pharmacology. 2022;13:869794.
16. Schagatay E, Lunde A, Nilsson S, Palm O, Lodin-Sundstrom A. Spleen contraction elevates hemoglobin concentration at high altitude during rest and exercise. Eur J Appl Physiol. 2020;120(12):2693-704.
17. Khairullah S, Jackson N. Markers of ineffective erythropoiesis in non-transfusion dependent β-thalassaemia. Med J Malaysia. 2021;76(1):41-5.
18. Alafi MH, Cook SF. Role of the spleen in acclimatization to hypoxia. Am J

621 Physiol. 1956;186(2):369-72.
622 19. Richardson M, Lodin A, Reimers J, Schagatay E. Short-term effects of
623 normobaric hypoxia on the human spleen. European journal of applied
624 physiology. 2008;104(2):395-9.
625 20. Lin HJ, Wang CT, Niu KC, Gao C, Li Z, Lin MT, et al. Hypobaric hypoxia
626 preconditioning attenuates acute lung injury during high-altitude exposure in
627 rats via up-regulating heat-shock protein 70. Clin Sci (Lond). 2011;121(5):223-
628 31.
629 21. Brent MB, Emmanuel T, Simonsen U, Bruel A, Thomsen JS. Hypobaric
630 hypoxia deteriorates bone mass and strength in mice. Bone. 2022;154:116203.
631 22. Holmstrom PK, Bird JD, Thrall SF, Kalker A, Herrington BA, Soriano JE, et al.
632 The effects of high altitude ascent on splenic contraction and the diving
633 response during voluntary apnoea. Exp Physiol. 2021;106(1):160-74.
634 23. Holmstrom P, Mulder E, Starfelt V, Lodin-Sundstrom A, Schagatay E. Spleen
635 Size and Function in Sherpa Living High, Sherpa Living Low and Nepalese
636 Lowlanders. Front Physiol. 2020;11:647.
637 24. Pernett F, Schagatay F, Vildevi C, Schagatay E. Spleen Contraction During
638 Sudden Eupneic Hypoxia Elevates Hemoglobin Concentration. Front Physiol.
639 2021;12:729123.
640 25. Wang Z, Tenzing N, Xu Q, Liu H, Ye Y, Wen Y, et al. Apoptosis is one cause of
641 thrombocytopenia in patients with high-altitude polycythemia. Platelets.
642 2023;34(1):2157381.
643 26. Pivkin IV, Peng Z, Karniadakis GE, Buffet PA, Dao M, Suresh S. Biomechanics
644 of red blood cells in human spleen and consequences for physiology and disease.
645 Proc Natl Acad Sci U S A. 2016;113(28):7804-9.
646 27. Wynn TA, Chawla A, Pollard JW. Macrophage biology in development,
647 homeostasis and disease. Nature. 2013;496(7446):445-55.
648 28. Gammella E, Buratti P, Cairo G, Recalcati S. Macrophages: central regulators
649 of iron balance. Metallomics. 2014;6(8):1336-45.
650 29. Zhihua Y, Yulin T, Yibo W, Wei D, Yin C, Jiahao X, et al. Hypoxia decreases
651 macrophage glycolysis and M1 percentage by targeting microRNA-30c and
652 mTOR in human gastric cancer. Cancer Sci. 2019;110(8):2368-77.
653 30. Zhang L, Patel S, Soulakova JN, Caldwell CC, St Pierre Schneider B. Mild
654 hypobaric hypoxia influences splenic proliferation during the later phase of
655 stress erythropoiesis. Exp Biol Med (Maywood). 2022;247(6):509-18.
656 31. Bellomo A, Mondor I, Spinelli L, Lagueyrie M, Stewart BJ, Brouilly N, et al.
657 Reticular Fibroblasts Expressing the Transcription Factor WT1 Define a
658 Stromal Niche that Maintains and Replenishes Splenic Red Pulp Macrophages.
659 Immunity. 2020;53(1):127-42 e7.
660 32. Lewis C, Murdoch C. Macrophage responses to hypoxia: implications for tumor
661 progression and anti-cancer therapies. Am J Pathol. 2005;167(3):627-35.
662 33. Henze AT, Mazzone M. The impact of hypoxia on tumor-associated
663 macrophages. J Clin Invest. 2016;126(10):3672-9.
664 34. Vijayan V, Wagener F, Immenschuh S. The macrophage heme-heme oxygenase-

1 system and its role in inflammation. Biochem Pharmacol. 2018;153:159-67.
35. Kovtunovych G, Eckhaus MA, Ghosh MC, Ollivierre-Wilson H, Rouault TA. Dysfunction of the heme recycling system in heme oxygenase 1-deficient mice: effects on macrophage viability and tissue iron distribution. Blood. 2010;116(26):6054-62.
36. Lee PJ, Jiang BH, Chin BY, Iyer NV, Alam J, Semenza GL, et al. Hypoxia-inducible factor-1 mediates transcriptional activation of the heme oxygenase-1 gene in response to hypoxia. J Biol Chem. 1997;272(9):5375-81.
37. Dawn B, Bolli R. HO-1 induction by HIF-1: a new mechanism for delayed cardioprotection? Am J Physiol Heart Circ Physiol. 2005;289(2):H522-4.
38. Anand RJ, Gribar SC, Li J, Kohler JW, Branca MF, Dubowski T, et al. Hypoxia causes an increase in phagocytosis by macrophages in a HIF-1alpha-dependent manner. J Leukoc Biol. 2007;82(5):1257-65.
39. Korolnek T, Hamza I. Macrophages and iron trafficking at the birth and death of red cells. Blood. 2015;125(19):2893-7.
40. Hamza I, Dailey HA. One ring to rule them all: Trafficking of heme and heme synthesis intermediates in the metazoans. Bba-Mol Cell Res. 2012;1823(9):1617-32.
41. Soares MP, Hamza I. Macrophages and Iron Metabolism. Immunity. 2016;44(3):492-504.
42. Ganz T. Macrophages and Iron Metabolism. Microbiol Spectr. 2016;4(5).
43. Dixon SJ, Lemberg KM, Lamprecht MR, Skouta R, Zaitsev EM, Gleason CE, et al. Ferroptosis: An Iron-Dependent Form of Nonapoptotic Cell Death. Cell. 2012;149(5):1060-72.
44. Zhang P, Chen L, Zhao QQ, Du XX, Bi MX, Li Y, et al. Ferroptosis was more initial in cell death caused by iron overload and its underlying mechanism in Parkinson's disease. Free Radical Bio Med. 2020;152:227-34.
45. Chen X, Yu CH, Kang R, Tang DL. Iron Metabolism in Ferroptosis. Front Cell Dev Biol. 2020;8.
46. Fuhrmann DC, Mondorf A, Beifuss J, Jung M, Brune B. Hypoxia inhibits ferritinophagy, increases mitochondrial ferritin, and protects from ferroptosis. Redox Biol. 2020;36:101670.
47. Youssef LA, Rebbaa A, Pampou S, Weisberg SP, Stockwell BR, Hod EA, et al. Increased erythrophagocytosis induces ferroptosis in red pulp macrophages in a mouse model of transfusion. Blood. 2018;131(23):2581-93.
48. Xie Y, Hou W, Song X, Yu Y, Huang J, Sun X, et al. Ferroptosis: process and function. Cell Death Differ. 2016;23(3):369-79.
49. Gao M, Yi J, Zhu J, Minikes AM, Monian P, Thompson CB, et al. Role of Mitochondria in Ferroptosis. Mol Cell. 2019;73(2):354-63 e3.

706 ## Figure legends

707 **Fig.1** HH exposure promotes erythrocytosis in mice. The C57BL/6 mice were treated
708 with normobaric normoxia (NN) and hypobaric hypoxia (HH) for 3, 7 and 14 days, and
709 blood was collected for the following tests. (**A**) Observation of the number and
710 morphology of RBCs by blood cell smear. Routine blood analysis of RBC counts (**B**)
711 and HGB (**C**), HCT (**D**), and MCH content (**E**). (**F**) Representative dot plots (one of
712 three experiments) of TO-positive cells (reticulocytes) in total populations of spleen.
713 (**G**) CD47 staining in splenic cells was analysed by flow cytometry. Representative dot
714 plots (one of three experiments) of CD47 expression after HH for 7 (**H**) and 14 (**I**) days
715 in total populations of the spleen. Data were expressed as the means ± SEM (n = 5 per
716 group); * $P < 0.05$, ** $P < 0.01$, *** $P < 0.001$ versus the NN group or the indicated
717 group.

718

719 **Fig. 2** The spleen plays an important role in suppressing the immoderate increase in
720 RBCs under HH conditions. C57BL/6 mice with or without splenectomy were treated
721 with NN and HH for different numbers of days, and the spleen and blood were collected
722 for subsequent analyses. (**A**) Morphological observation, (**B**) spleen volume and (**C**)
723 spleen weight detection after HH exposure. (**D-H**) Blood observation and
724 hematological index detection. Data were expressed as the means ± SEM (n = 9 per
725 group); * $P < 0.05$, ** $P < 0.01$, *** $P < 0.001$ versus the NN group or the indicated
726 group.

727

728 **Fig. 3** HH exposure causes a decrease in the number of macrophages in spleen. The
729 C57BL/6 mice were treated with NN and HH for 7 or 14 days, and the spleen and blood
730 were collected for subsequent detection. (**A**) Visualization of spleen cell clusters using
731 uniform manifold approximation and projection (UMAP). Each color represents a
732 cluster of specific cells of the spleen, which was identified by a defined gene expression
733 profile. (**B**) The proportions of different macrophage clusters derived from either NN-
734 or HH-treated mouse spleens were analysed. (**C**) Individual macrophages derived from
735 either NN- or HH-treated mouse spleens are denoted. (**D**) Calcein/PI double staining
736 was analysed by flow cytometry. (**E and F**) Cell death proportions in total splenic cells
737 are given as bar graphs. (**G** and **J**) Western blot detecting CD16 and CD206 protein
738 expression in the spleen. (**H-I** and **K-L**) Statistical analysis of CD16 and CD206
739 expression in H and K. (**M**) F4/80 staining with CD11b, CD86 or CD206 in splenic
740 cells was analysed by flow cytometry. (**N**) qPCR analysis of CCL2 and CCL7
741 expression in the spleen. (**O**) qPCR analysis of Csf1 and Csf2 expression in the spleen.
742 (**P**) Flow cytometry detection of CD111b and Ly6C double-stained cells in the BM and
743 spleen. $CD11b^{hi}Ly6C^{hi}$ cell proportions in the BM (**Q-R**) and spleen (**S-T**) are given as
744 bar graphs. (**U**) HO-1 and F4/80 expression in the spleen after HH exposure for 7 and
745 14 days. Data were expressed as the means ± SEM (n = 3 per group); * $P < 0.05$, ** P
746 < 0.01, *** $P < 0.001$ versus the NN group or the indicated group.
747
748 **Fig. 4** HH exposure decreases erythrophagocytosis and iron processing capacity in the
749 spleen. (**A**) *Ecoil* was labelled with Cy5.5 dye and photographed under a fluorescence

750 microscope. (**B**) The phagocytic activity of splenic cells for Cy5.5-labelled *Ecoil* in
751 vitro. (**C**) Autologous erythrocytes were labelled with biotin followed by NIH-FITC
752 detection and photographed under a fluorescence microscope. (**D**) Experimental
753 diagram of phagocytic activity in splenic cells after HH exposure in vivo. Flow
754 cytometry detection of FITC-stained cells in the blood (**E**) and spleen (**F**) after HH
755 exposure for 7 and 14 days. The FITC-positive cell proportions in the blood (**G**) and
756 spleen (**H**) are given as bar graphs. (**I**) Experimental design of C57Bl6 mice (n=3 per
757 group) treated at days 7 and 11 with a single intravenous injection of Tuftsin (1.5 mg/kg),
758 followed by HH exposure until day 14 for isolation of the spleen for F4/80
759 immunohistochemistry and iron staining. (**J**) F4/80 and iron staining in the spleen after
760 HH exposure for 14 days with Tuftsin treatment. (**K**) Quantitative results of F4/80
761 expression in the spleen described in (**J**). (**L**) Semiquantitative iron levels in the spleen
762 described in (**J**). Data were expressed as the means ± SEM (n = 3 per group); * $P <$
763 0.05, ** $P < 0.01$, *** $P < 0.001$ versus the NN group or the indicated group.
764
765 **Fig. 5** HH exposure promotes iron mobilization and induces ferroptosis in the spleen.
766 The C57BL/6 mice were treated with NN and HH for 7 days, and the spleen was
767 collected for subsequent detection. (**A**) Western blot detection of HO-1, Ft-L, Ft-H,
768 NCOA4, Fpn and TfR protein expression in spleen. (**B**) Statistical analysis of HO-1,
769 Ft-L, Ft-H, NCOA4, Fpn and TfR protein expression in A. (**C**) GEO data analysis of
770 HMOX1, FTL, FTH1, NCOA4, SLC40A1, and TFRC mRNA expression in PMBCs
771 before and after climbing to high altitude (n=98). (**D**) Western blot detection of ACSL4,

772 GPX4 and xCT protein expression in the spleen. (**E**) Statistical analysis of ACSL4,
773 GPX4 and xCT protein expression in D. (**F**) GEO data analysis of ACSL4, GPX4 and
774 SLC7A11 mRNA expression in PMBCs before and after climbing to high altitude
775 (n=98). (**G**) The content of Fe^{2+} in the spleen was detected using the FerroFarRed probe
776 by flow cytometry. (**H**) The level of lipid ROS in the spleen was detected using the
777 C11-BODIPY probe by flow cytometry. The MDA (**I**), Cys (**J**) and GSH (**K**) levels in
778 the spleen were detected using biochemical detection kits. Data were expressed as the
779 means ± SEM (n = 3 per group); * $P < 0.05$, ** $P < 0.01$, *** $P < 0.001$ versus the NN
780 group or the indicated group.
781
782 **Fig. 6** Hypoxia promoted primary peritoneal macrophage ferroptosis. Primary
783 peripheral macrophages were cultured under 1% hypoxia for different times (0, 12, 24,
784 48 h) with or without pre-treatment with 10 μM Fer-1 for 1 h, and then the cells were
785 collected for subsequent detection. (**A**) Immunofluorescence detection of Fe^{2+} levels in
786 macrophages after hypoxia exposure for 24 h using the FerroFarRed probe under a
787 fluorescence microscope. (**B**) Quantitative results of fluorescence intensity in the
788 macrophages described in **A**. (**C**) Flow cytometry detection of Fe^{2+} levels in
789 macrophages exposed to hypoxia for 24 h using the FerroFarRed probe. (**D**)
790 Immunofluorescence detection of lipid ROS levels in macrophages exposed to hypoxia
791 for 24 h using the C11-BODIPY probe under a fluorescence microscope. (**E**)
792 Quantitative results of mean fluorescence intensity in the macrophages described in **D**.
793 (**F**) Western blot detection of ACSL4, GPX4 and xCT protein expression in

macrophages under hypoxia for different times. (**G**) Calcein/PI double staining in macrophages after 24 h of exposure to hypoxia was analysed by flow cytometry. (**H**) Cell death proportions in macrophages are given as bar graphs. (**I**) Macrophage phagocytic activity of Cy5.5-labelled *Ecoil* after 24 h of hypoxia exposure by flow cytometry in vitro. (**J**) Immunofluorescence detection of Fe^{2+} levels in macrophages pre-treated with Fer-1 followed by 24 h of hypoxia exposure using the FerroFarRed probe. (**K**) Quantitative results of fluorescence intensity in the macrophages described in **J**. (**L**) Western blot detection of ACSL4, GPX4 and xCT protein expression in macrophages pre-treated with Fer-1 followed by 24 h of hypoxia exposure. (**M** and **N**) Statistical analysis of ACSL4, GPX4 and xCT protein expression in **L**. MDA (**P**), Cys (**Q**), and GSH (**R**) levels in macrophages pre-treated with Fer-1 followed by 24 h of hypoxia exposure were detected using kits by biochemical methods. Data were expressed as the means ± SEM (n = 3 per group); * $P < 0.05$, ** $P < 0.01$, *** $P < 0.001$ versus the NN group or the indicated group.

Fig. 7 High altitude/hypobaric hypoxia exposure inhibits erythrophagocytosis by inducing ferroptosis in macrophages in the spleen. HA/HH exposure induces iron mobilization, especially increased Fe^{2+} levels, which are further increased in the spleen/macrophages of mice. On the other hand, HA/HH exposure increased ACSL4 expression and inhibited GSH production by suppressing xCT expression and GSH production. The above results enhance lipid peroxidation and further macrophage ferroptosis. Meanwhile, HA/HH exposure decreases monocyte migration and

differentiation from the BM to the spleen. Taken together, HA/HH exposure inhibits erythrophagocytosis and further promotes erythrocytosis, which may aggravate HAPC development.

Supplementary Figure S1. HH exposure promotes iron mobilization and induces ferroptosis in the spleen. The C57BL/6 mice were treated with NN and HH for 14 days, and the spleen was collected for subsequent detection. (**A**) Western blot detection of HO-1, Ft-L, Ft-H, NCOA4, Fpn and TfR protein expression in spleen. (**B**) Statistical analysis of HO-1, Ft-L, Ft-H, NCOA4, Fpn and TfR protein expression in **A**. (**C**) Western blot detection of ACSL4, GPX4 and xCT protein expression in the spleen. (**D**) Statistical analysis of ACSL4, GPX4 and xCT protein expression in **C**. (**E**) The content of Fe^{2+} in the spleen was detected using the FerroFarRed probe by flow cytometry. (**F**) Quantitative results of the mean fluorescence intensity in **E**. (**G**) The level of lipid ROS in the spleen was detected using the C11-BODIPY probe by flow cytometry. (**H**) Quantitative results of the mean fluorescence intensity in **G**. (**I**) MDA, (**J**) Cys, and (**K**) GSH levels in the spleen were detected using kits by biochemical methods. Data were expressed as the means ± SEM (n = 3 per group); * $P < 0.05$, ** $P < 0.01$, *** $P < 0.001$ versus the NN group or the indicated group.

Fig.1

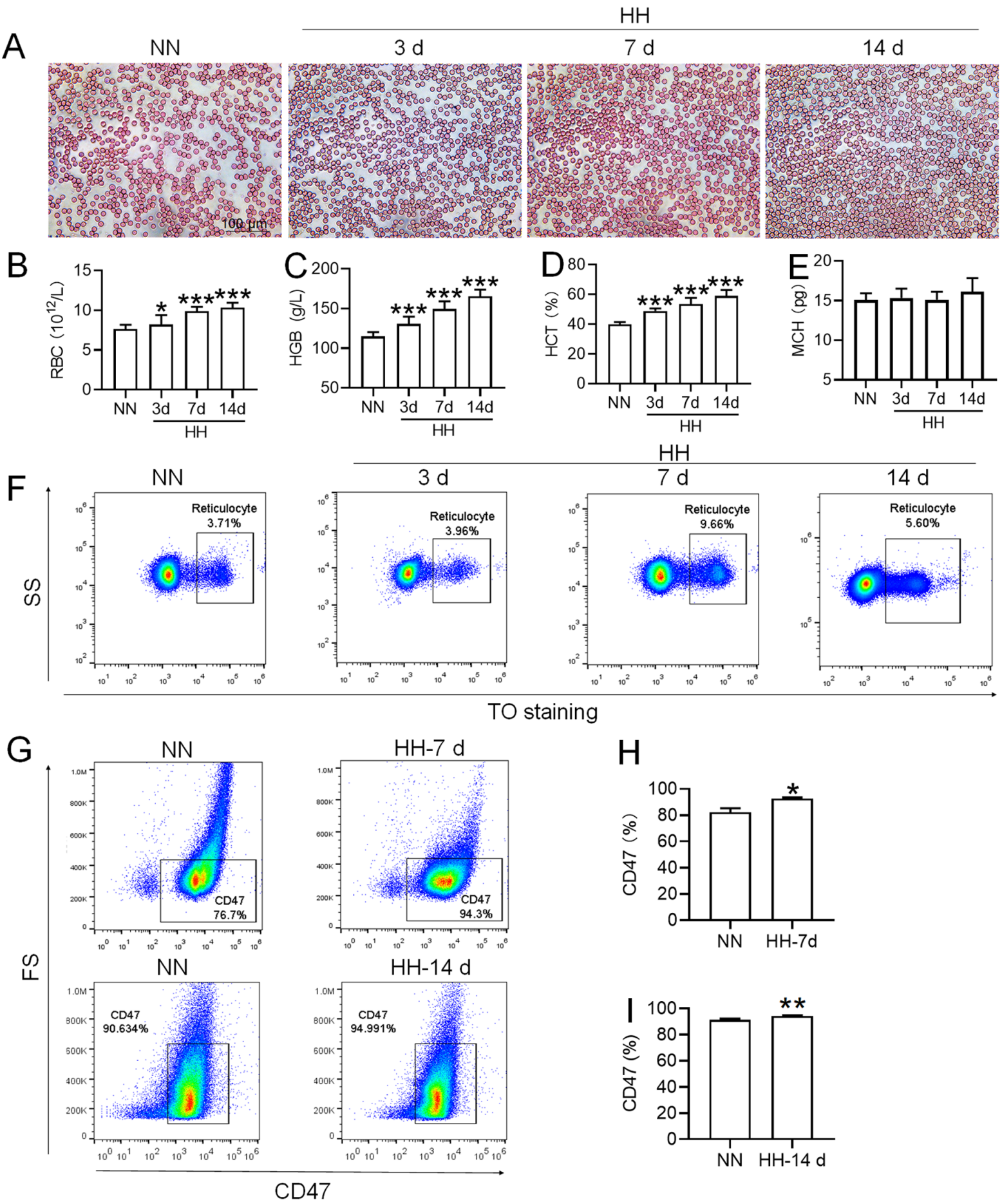
A
HH
NN
3 d
7 d
14 d
100 μm
B
RBC (10^12/L)
NN 3d 7d 14d
HH
C
HGB (g/L)
D
HCT (%)
E
MCH (pg)
F
Reticulocyte 3.71%
Reticulocyte 3.96%
Reticulocyte 9.66%
Reticulocyte 5.60%
SS
TO staining
G
HH-7 d
HH-14 d
CD47 76.7%
CD47 94.3%
CD47 90.634%
CD47 94.991%
FS
CD47
H
CD47 (%)
NN HH-7d
I
NN HH-14 d

Fig.2

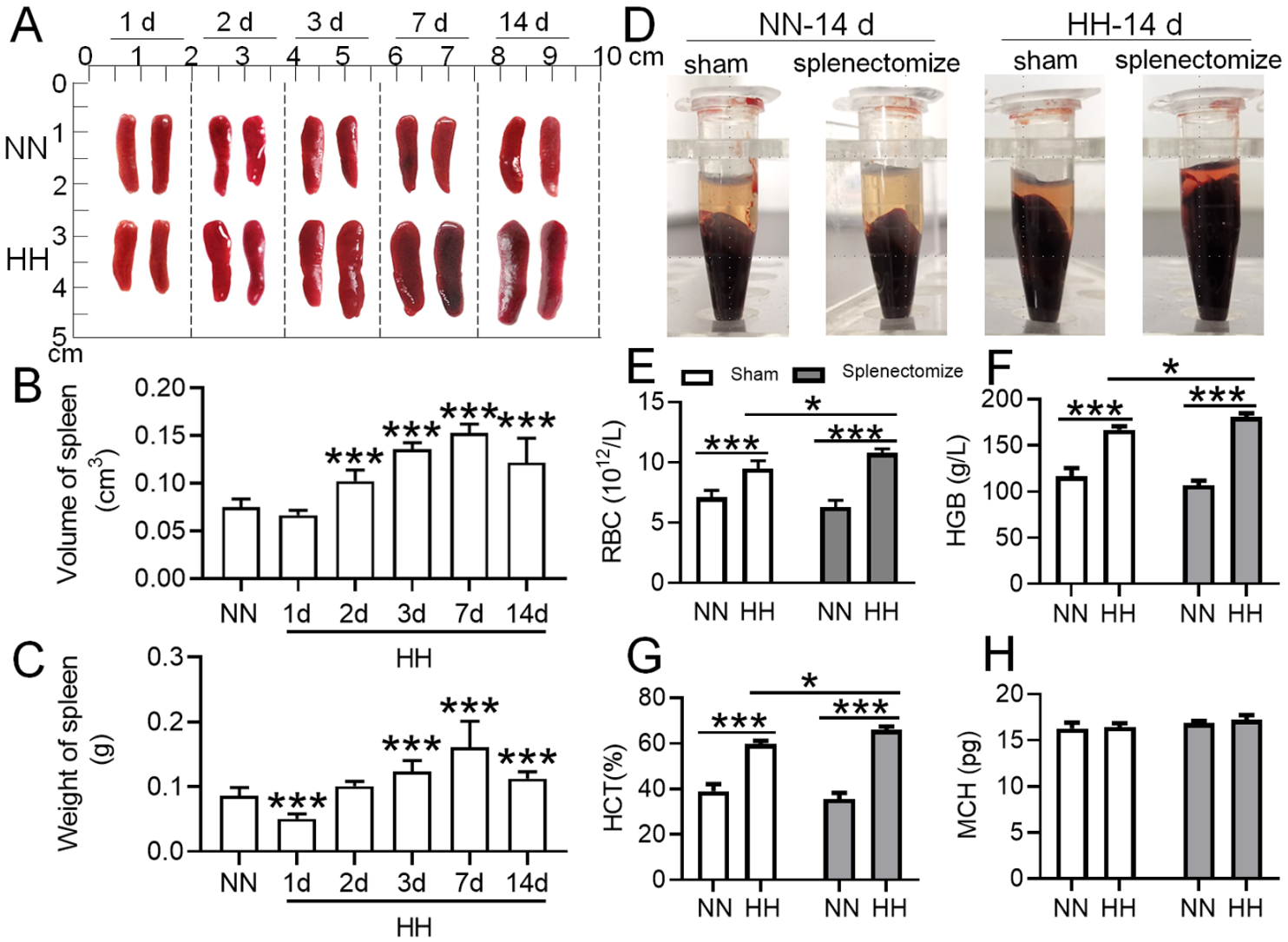
A
1 d
2 d
3 d
7 d
14 d
0 1 2 3 4 5 6 7 8 9 10 cm
NN
HH
cm
B
Volume of spleen (cm3)
0.20
0.15
0.10
0.05
0.00
***
NN 1d 2d 3d 7d 14d
HH
C
Weight of spleen (g)
0.3
0.2
0.1
0.0
***
NN 1d 2d 3d 7d 14d
HH
D
NN-14 d
HH-14 d
sham
splenectomize
sham
splenectomize
E
Sham
Splenectomize
RBC (10^12/L)
15
10
5
0
*
***
NN HH NN HH
F
HGB (g/L)
200
150
100
50
0
*
***
NN HH NN HH
G
HCT(%)
80
60
40
20
0
*
***
NN HH NN HH
H
MCH (pg)
20
15
10
5
0
NN HH NN HH

Fig.3

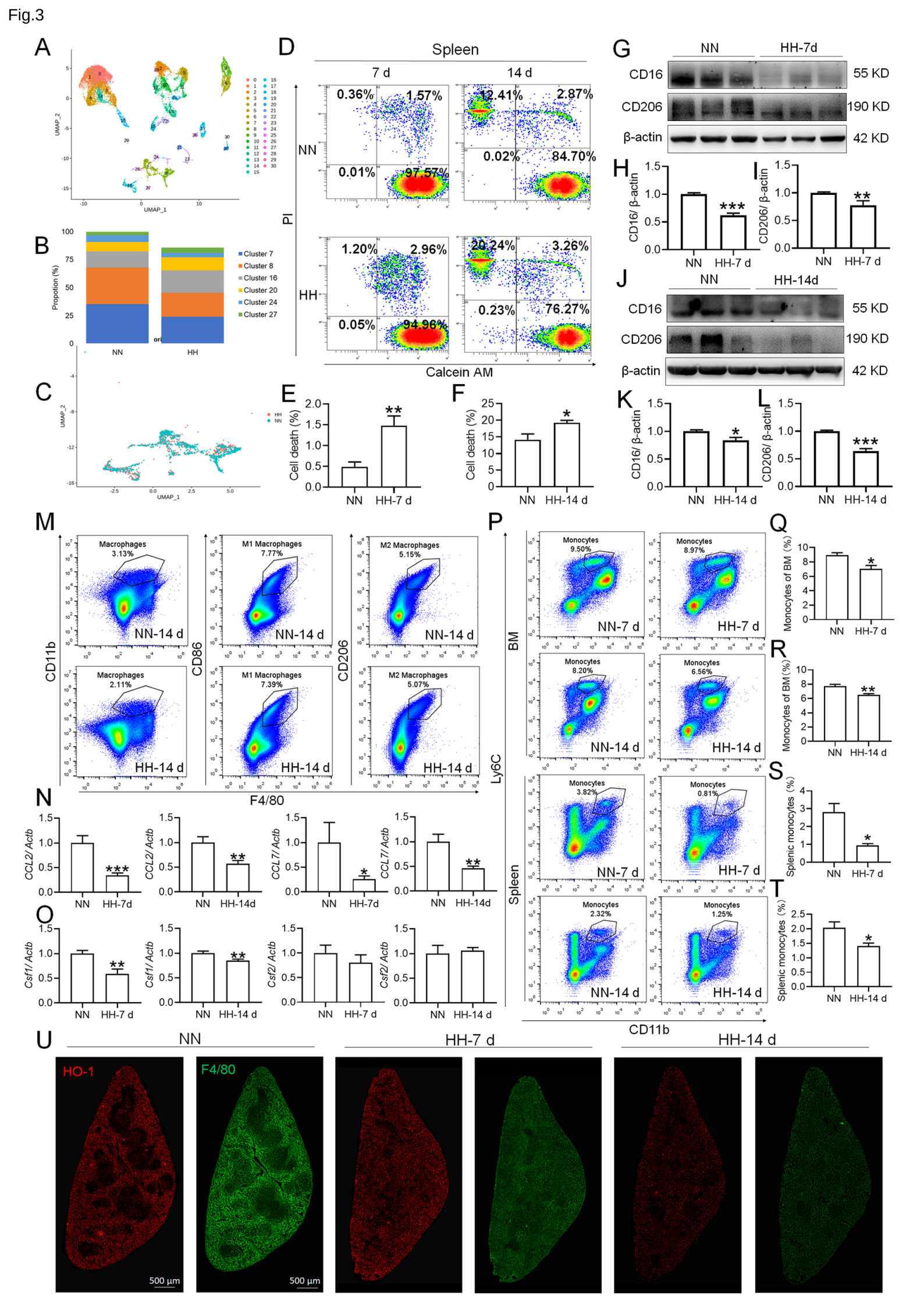
A
UMAP_1
UMAP_2
B
Propotion (%)
Cluster 7
Cluster 8
Cluster 16
Cluster 20
Cluster 24
Cluster 27
NN
HH
C
D
Spleen
7 d
14 d
NN
HH
PI
Calcein AM
0.36%
1.57%
0.01%
97.57%
12.41%
2.87%
0.02%
84.70%
1.20%
2.96%
0.05%
94.96%
20.24%
3.26%
0.23%
76.27%
E
Cell death (%)
NN
HH-7 d
F
Cell death (%)
NN
HH-14 d
G
NN
HH-7d
CD16
CD206
β-actin
55 KD
190 KD
42 KD
H
CD16/ β-actin
NN
HH-7 d
I
CD206/ β-actin
NN
HH-7 d
J
NN
HH-14d
CD16
CD206
β-actin
55 KD
190 KD
42 KD
K
CD16/ β-actin
NN
HH-14 d
L
CD206/ β-actin
NN
HH-14 d
M
Macrophages
3.13%
NN-14 d
Macrophages
2.11%
HH-14 d
M1 Macrophages
7.77%
NN-14 d
M1 Macrophages
7.39%
HH-14 d
M2 Macrophages
5.15%
NN-14 d
M2 Macrophages
5.07%
HH-14 d
CD11b
CD86
CD206
F4/80
N
CCL2/ Actb
NN
HH-7d
CCL2/ Actb
NN
HH-14d
CCL7/ Actb
NN
HH-7d
CCL7/ Actb
NN
HH-14d
O
Csf1/ Actb
NN
HH-7 d
Csf1/ Actb
NN
HH-14 d
Csf2/ Actb
NN
HH-7 d
Csf2/ Actb
NN
HH-14 d
P
BM
Spleen
Ly6C
CD11b
Monocytes
9.50%
NN-7 d
Monocytes
8.97%
HH-7 d
Monocytes
8.20%
NN-14 d
Monocytes
6.56%
HH-14 d
Monocytes
3.82%
NN-7 d
Monocytes
0.81%
HH-7 d
Monocytes
2.32%
NN-14 d
Monocytes
1.25%
HH-14 d
Q
Monocytes of BM (%)
NN
HH-7 d
R
Monocytes of BM (%)
NN
HH-14 d
S
Splenic monocytes (%)
NN
HH-7 d
T
Splenic monocytes (%)
NN
HH-14 d
U
NN
HH-7 d
HH-14 d
HO-1
F4/80
500 μm
500 μm

Fig.4

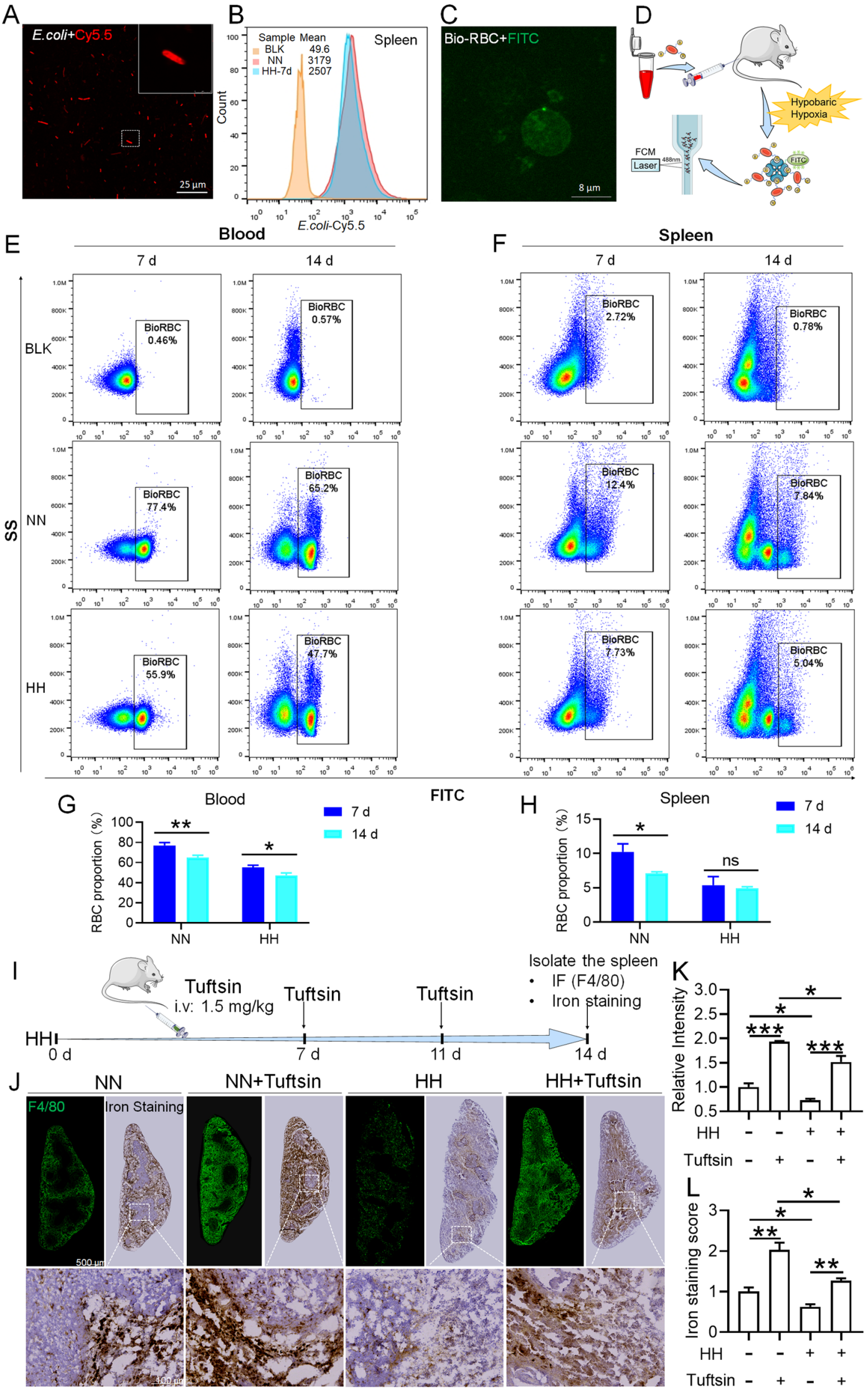
A
E.coli+Cy5.5
25 μm
B
Sample Mean
BLK 49.6
NN 3179
HH-7d 2507
Spleen
Count
E.coli-Cy5.5
C
Bio-RBC+FITC
8 μm
D
Hypobaric Hypoxia
FCM
Laser
488nm
FITC
E
Blood
7 d
14 d
BLK
NN
HH
SS
BioRBC 0.46%
BioRBC 0.57%
BioRBC 77.4%
BioRBC 65.2%
BioRBC 55.9%
BioRBC 47.7%
F
Spleen
BioRBC 2.72%
BioRBC 0.78%
BioRBC 12.4%
BioRBC 7.84%
BioRBC 7.73%
BioRBC 5.04%
FITC
G
Blood
RBC proportion (%)
7 d
14 d
NN
HH
H
Spleen
ns
I
Tuftsin
i.v: 1.5 mg/kg
Tuftsin
Tuftsin
Isolate the spleen
IF (F4/80)
Iron staining
HH
0 d
7 d
11 d
14 d
J
NN
NN+Tuftsin
HH
HH+Tuftsin
F4/80
Iron Staining
500 μm
K
Relative Intensity
HH
Tuftsin
L
Iron staining score
HH
Tuftsin

Fig.5

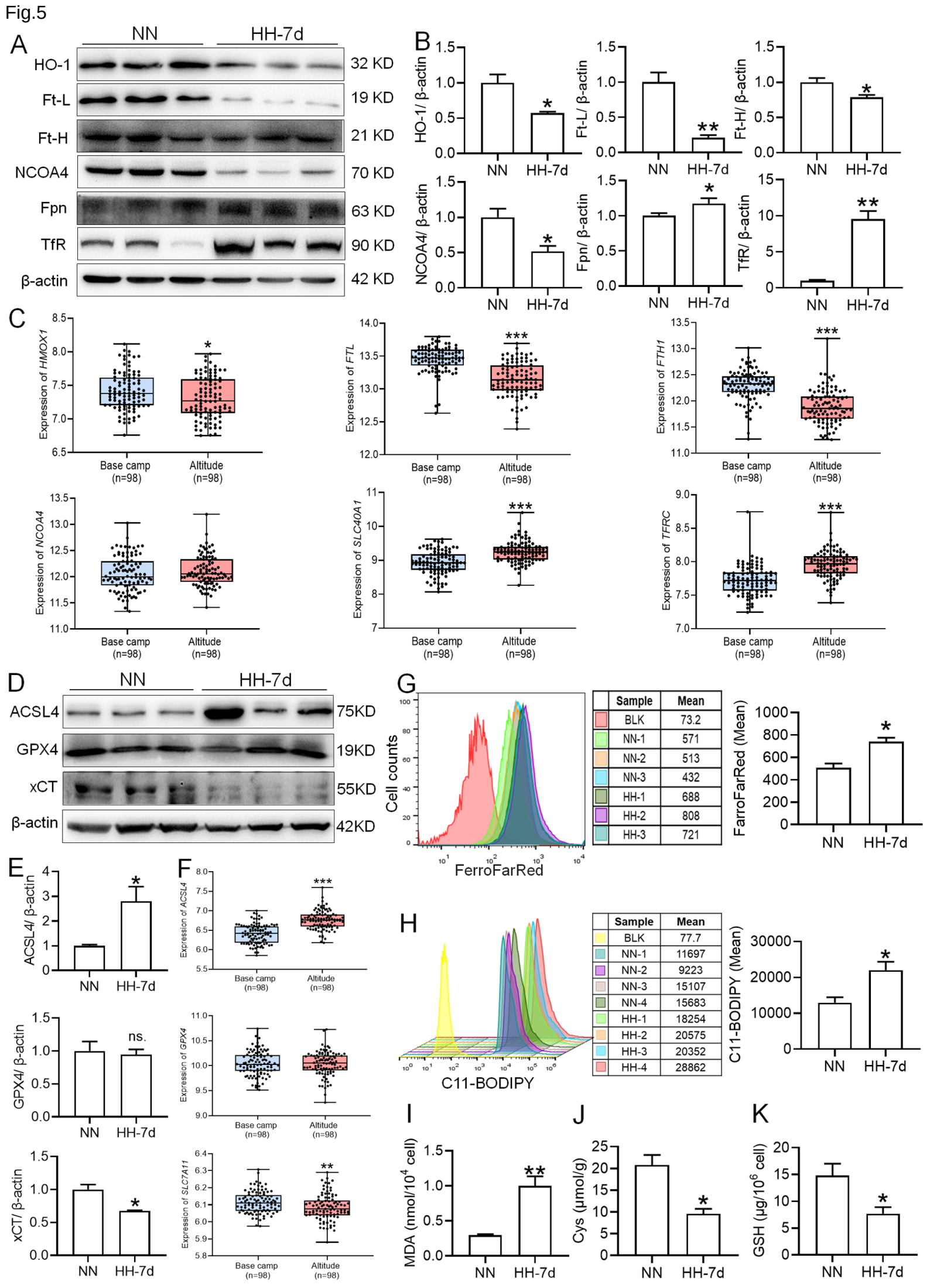
A
NN
HH-7d
HO-1
Ft-L
Ft-H
NCOA4
Fpn
TfR
β-actin
32 KD
19 KD
21 KD
70 KD
63 KD
90 KD
42 KD
B
HO-1/ β-actin
Ft-L/ β-actin
Ft-H/ β-actin
NCOA4/ β-actin
Fpn/ β-actin
TfR/ β-actin
C
Expression of HMOX1
Expression of FTL
Expression of FTH1
Expression of NCOA4
Expression of SLC40A1
Expression of TFRC
Base camp (n=98)
Altitude (n=98)
D
ACSL4
GPX4
xCT
β-actin
75KD
19KD
55KD
42KD
E
ACSL4/ β-actin
GPX4/ β-actin
xCT/ β-actin
ns.
F
Expression of ACSL4
Expression of GPX4
Expression of SLC7A11
G
Cell counts
FerroFarRed
FarroFarRed (Mean)
Sample | Mean
BLK | 73.2
NN-1 | 571
NN-2 | 513
NN-3 | 432
HH-1 | 688
HH-2 | 808
HH-3 | 721
H
C11-BODIPY
C11-BODIPY (Mean)
Sample | Mean
BLK | 77.7
NN-1 | 11697
NN-2 | 9223
NN-3 | 15107
NN-4 | 15683
HH-1 | 18254
HH-2 | 20575
HH-3 | 20352
HH-4 | 28862
I
MDA (nmol/10^4 cell)
J
Cys (μmol/g)
K
GSH (μg/10^6 cell)

Fig.6

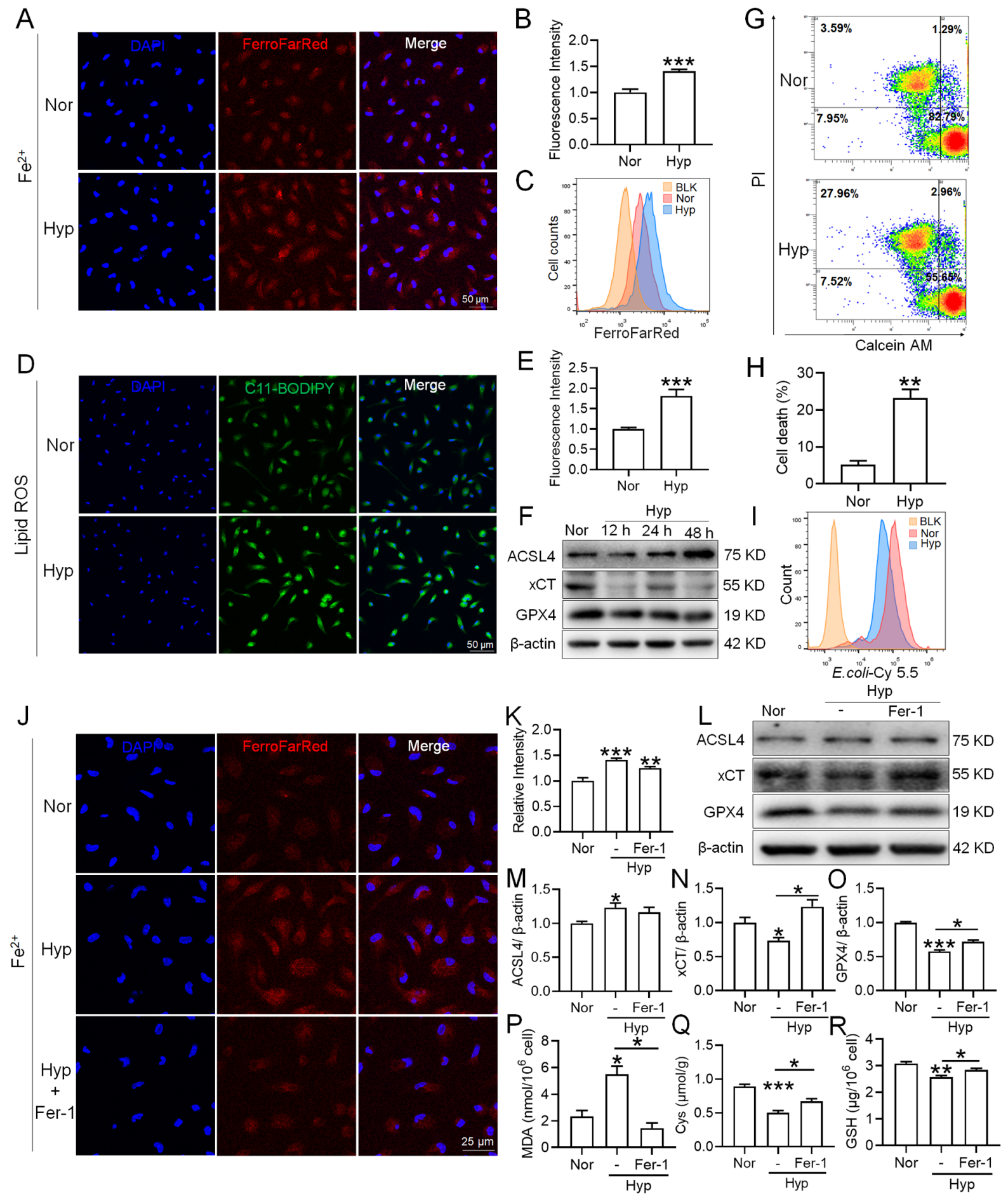
A
DAPI
FerroFarRed
Merge
Nor
Hyp
Fe2+
50 μm
B
Fluorescence Intensity
Nor
Hyp
C
BLK
Nor
Hyp
Cell counts
FerroFarRed
G
3.59%
1.29%
7.95%
82.79%
27.96%
2.96%
7.52%
55.65%
PI
Calcein AM
D
DAPI
C11-BODIPY
Merge
Lipid ROS
50 μm
E
Fluorescence Intensity
H
Cell death (%)
F
Nor
12 h
24 h
48 h
ACSL4
xCT
GPX4
β-actin
75 KD
55 KD
19 KD
42 KD
I
Count
E.coli-Cy 5.5
J
DAPI
FerroFarRed
Merge
Hyp + Fer-1
25 μm
K
Relative Intensity
Fer-1
L
M
ACSL4/ β-actin
N
xCT/ β-actin
O
GPX4/ β-actin
P
MDA (nmol/10^6 cell)
Q
Cys (μmol/g)
R
GSH (μg/10^6 cell)

Fig.7

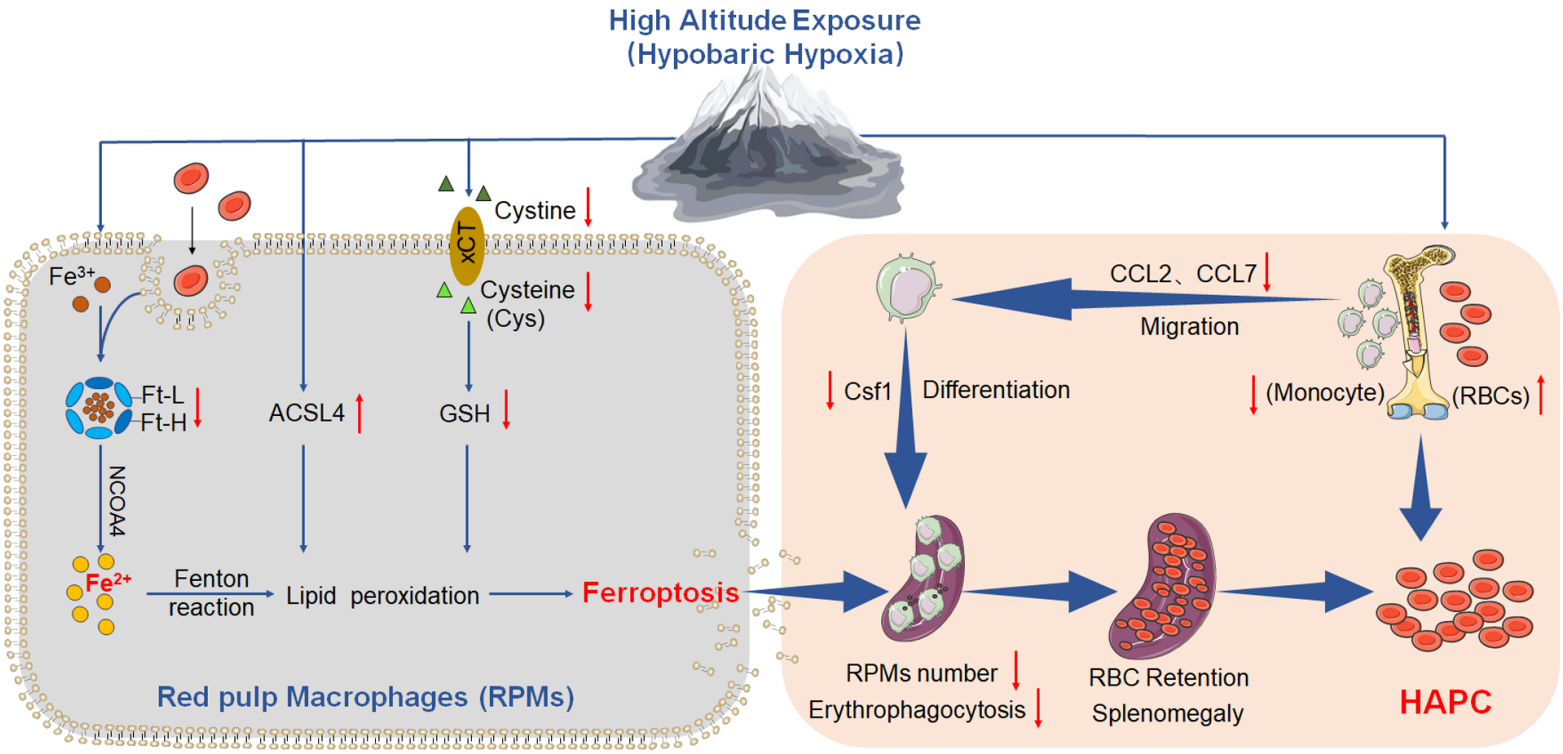
High Altitude Exposure
(Hypobaric Hypoxia)
Cystine
xCT
Cysteine
(Cys)
Fe3+
Ft-L
Ft-H
ACSL4
GSH
NCOA4
Fe2+
Fenton
reaction
Lipid peroxidation
Ferroptosis
Red pulp Macrophages (RPMs)
CCL2、CCL7
Migration
Csf1
Differentiation
(Monocyte)
(RBCs)
RPMs number
Erythrophagocytosis
RBC Retention
Splenomegaly
HAPC

Fig. S1

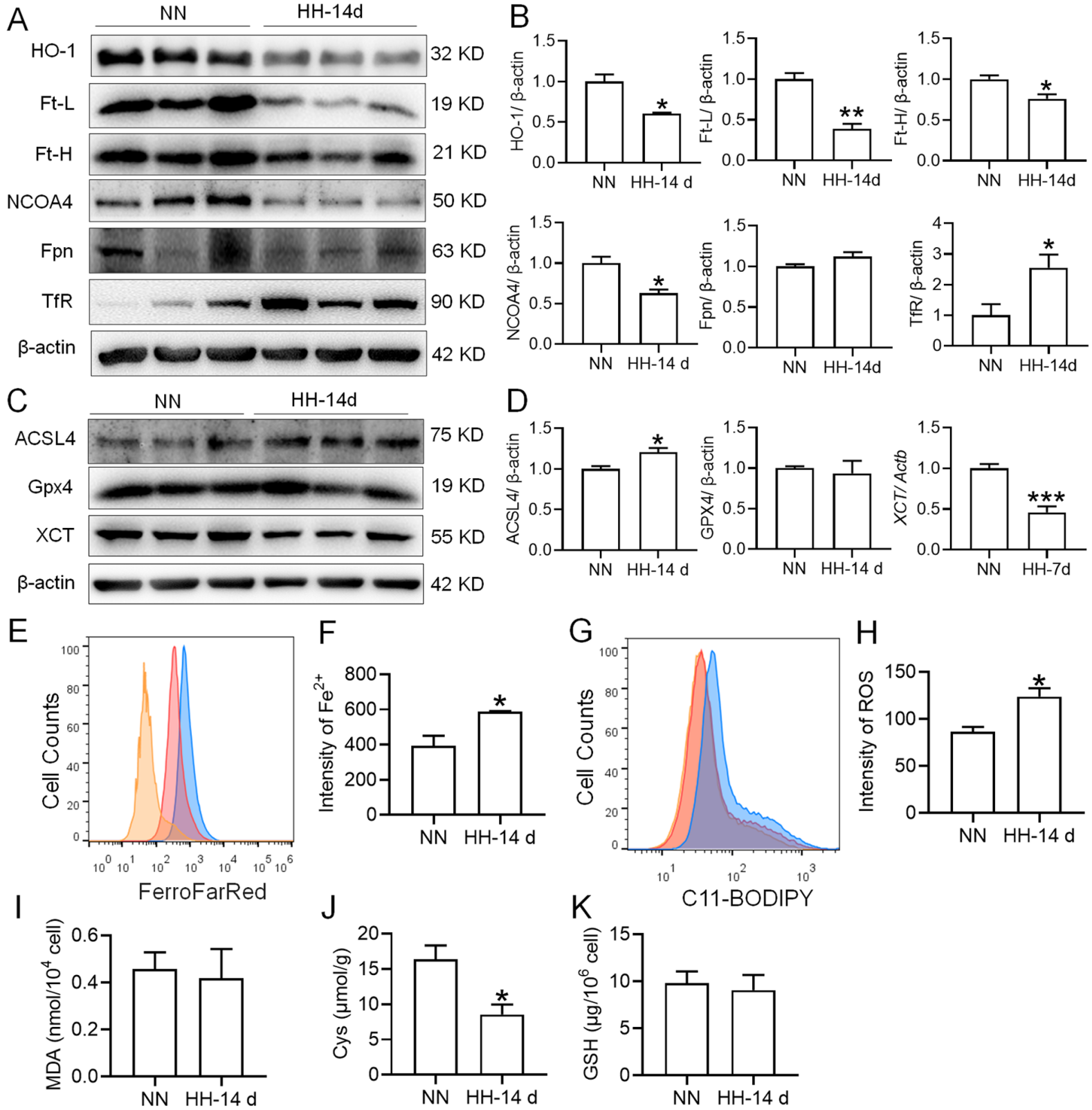
A
NN
HH-14d
HO-1
Ft-L
Ft-H
NCOA4
Fpn
TfR
β-actin
32 KD
19 KD
21 KD
50 KD
63 KD
90 KD
42 KD
B
HO-1/ β-actin
Ft-L/ β-actin
Ft-H/ β-actin
NCOA4/ β-actin
Fpn/ β-actin
TfR/ β-actin
NN
HH-14 d
HH-14d
C
ACSL4
Gpx4
XCT
β-actin
75 KD
19 KD
55 KD
42 KD
D
ACSL4/ β-actin
GPX4/ β-actin
XCT/ Actb
HH-7d
E
Cell Counts
FerroFarRed
F
Intensity of Fe2+
G
C11-BODIPY
H
Intensity of ROS
I
MDA (nmol/10^4 cell)
J
Cys (μmol/g)
K
GSH (μg/10^6 cell)